R&T 4124128

MATTER-WAVE INTERFEROMETRY WITH LASER COOLED ATOMS

David McIntyre

Department of Physics, Oregon State University, Corvallis, OR 97331-6507

DTIC
ELECTE
NOV 30 1993
A

I. Introduction

This research program is concerned with matter-wave interferometry of laser cooled atoms. A slow beam of laser cooled rubidium atoms will be used as the matter-wave source. The atom optical elements are microfabricated amplitude transmission gratings which will be used in a three-grating interferometer to split and recombine the rubidium beam. The atomic interferometer will be a useful new tool with which to perform precision experiments in atomic physics, quantum optics, and gravitation.

The research program takes advantage of three new technologies, the combination of which provides a unique opportunity to construct a compact and stable interferometer. The techniques of laser cooling and trapping are used to produce cold rubidium atoms in a well collimated beam. Commercially available diode lasers with optical feedback frequency stabilization are used for the laser cooling and trapping beams and for atomic beam diagnostics. Finally, submicron transmission gratings made with high-resolution electron-beam lithography are used as the coherent beam splitters of the atomic interferometer. Figure 1 shows the proposed interferometer geometry with the two paths that are generally used in such a device. The three-grating Bonse-Hart interferometer is a particularly useful design since it has intrinsically equal path lengths and is relatively insensitive to misalignments.[1,2] Figure 2 shows a schematic of our experiment in which the matter-wave source is a laser cooled rubidium atomic beam. A thermal beam of rubidium atoms is first slowed using chirped laser cooling.[3,4] The slow atoms drift into a two-
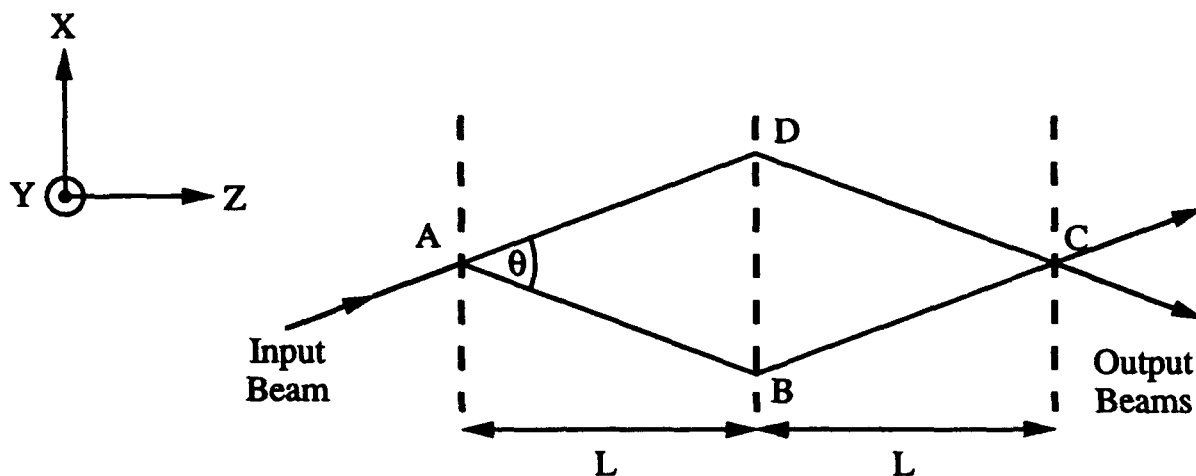
Fig. 1. Three-grating Bonse-Hart interferometer with two-path interference configuration shown.
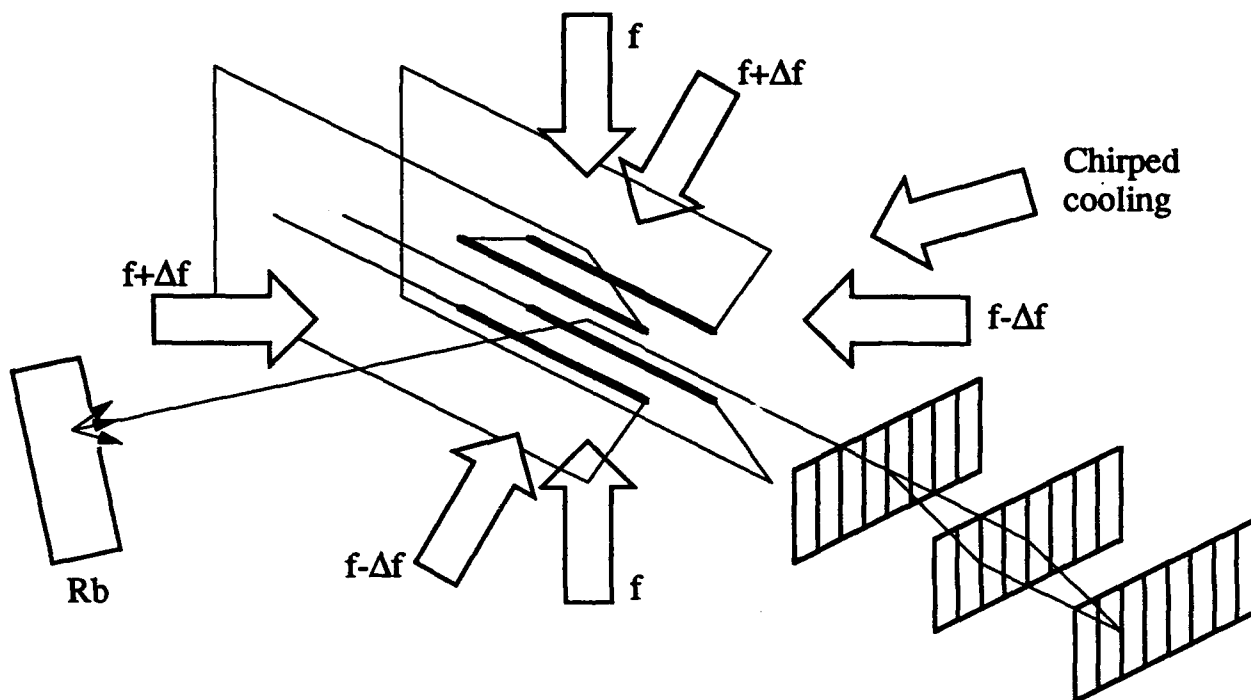

Fig. 2. Experimental schematic for three-grating interferometry with laser cooled atomic beam. The pieces of the magnetic field coils shown in bold are the ones mainly responsible for the two-dimensional quadrupole field forming the funnel.

dimensional magnetic quadrupole field in which six laser beams intersect to form a two-dimensional magneto-optic trap or so-called atomic funnel.[5] The atoms experience molasses-type damping in all three dimensions and are trapped in the two dimensions transverse to the axis of the trap. Along the axis of the trap, the atoms move with a velocity determined by the intersecting laser beam frequencies. We have planned for a mean atomic velocity of 10 m/s, corresponding to a de Broglie wavelength of 0.5 nm. The emerging atomic beam will have a temperature of approximately 500 μK, corresponding to a coherence length of 50 wavelengths. The beam will then enter the three-grating interferometer. The amplitude transmission gratings have a period of 250 nm and are made from free-standing silicon nitride films on silicon substrates.[6] The three gratings will be separated by 5 cm and will diffract the rubidium beam by 2 mrad into the first order. Compared to the other interferometers which have been demonstrated using material structures,[7] ours is relatively compact. The ability to tune the velocity of the funnel output beam also provides our experiment with another degree of flexibility.

In the 2 and three-quarters years since this project began, progress has taken place along several parallel fronts. We have constructed much of the apparatus and have produced the cooled atomic beam source. We are now working on characterizing the cold atomic beam and directing it into the atom interferometer.

II. Diode laser frequency stabilization

Our original diode-laser systems used optical-feedback stabilization from Fabry-Perot confocal cavities.[8,9] We have since redirected our efforts to building and using diode-laser systems that use diffraction gratings as the feedback element.[10] These lasers are simpler to implement and have comparable performance. Figure 3 shows a schematic of the laser system. A holographic grating at the Littrow angle provides the optical feedback. The laser diode, collimator lens, and grating are all mounted on a small aluminum block for mechanical and thermal stability. Residual mechanical vibrations of the extended cavity are reduced with a servo-control system that uses the diode-laser injection current to control the laser frequency. The electronic servo-control loop has a unity-gain frequency ($\approx$ 100 kHz) far above any mechanical resonances, so is very
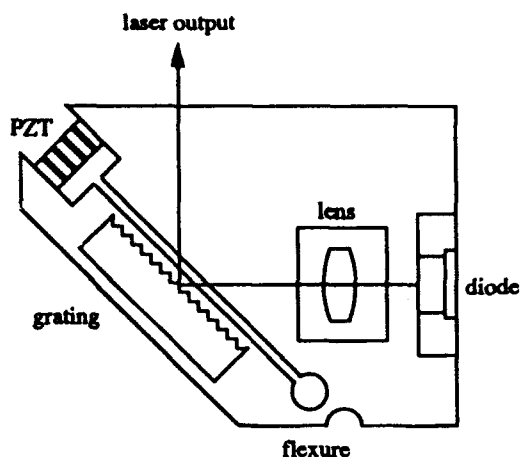
Fig. 3. Diagram of laser system with optical feedback from a diffraction grating. The grating is held with a commercial mirror mount which is not shown. The piezoelectric transducer (PZT) bends the flexure to tilt and translate the grating.
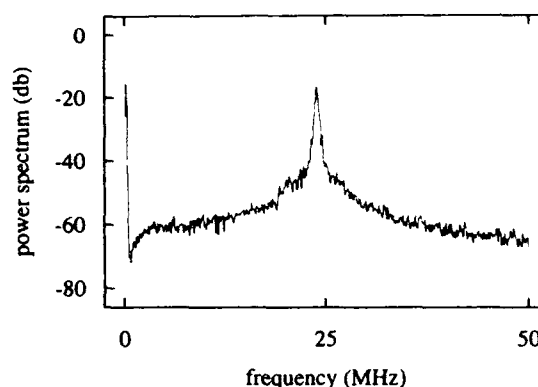
Fig. 4. Spectrum of the beat note between a grating-feedback laser and a cavity-feedback laser. The spectrum was taken with a 100 kHz resolution bandwidth.

effective at reducing the mechanical noise in the system. To characterize the linewidth of these laser systems we have performed heterodyne measurements between a grating-feedback laser and a narrow linewidth ($\approx$ 10 kHz) cavity-feedback laser.[8,9] We find the grating-feedback laser to have a FWHM linewidth of 150 kHz.

The needs of our experiment have lead us to use three different schemes to determine the diode laser frequencies. For the chirped cooling lasers we use a confocal Fabry-Perot etalon as the frequency discriminator. The laser can be scanned while it is locked to the etalon if the etalon length and the grating angle are synchronously ramped. The laser frequency used in a magneto-optic trap wants to be stabilized one to several linewidths ($\approx$ 5 - 20 MHz) below the trapping transition. We have found polarization spectroscopy to be useful in these situations as it provides a dispersive signal that is optimal for locking.[11] By adjusting the electronic offset in the servo-control circuit, the laser frequency can be locked over a range of approximately 60 MHz ($\approx$ +10 to -50 MHz). To produce the frequency shifted laser beams required in the atomic funnel, we have developed a simple electronic frequency discriminator that can be used to frequency-offset lock two lasers. The complete frequency-offset locking system is shown in
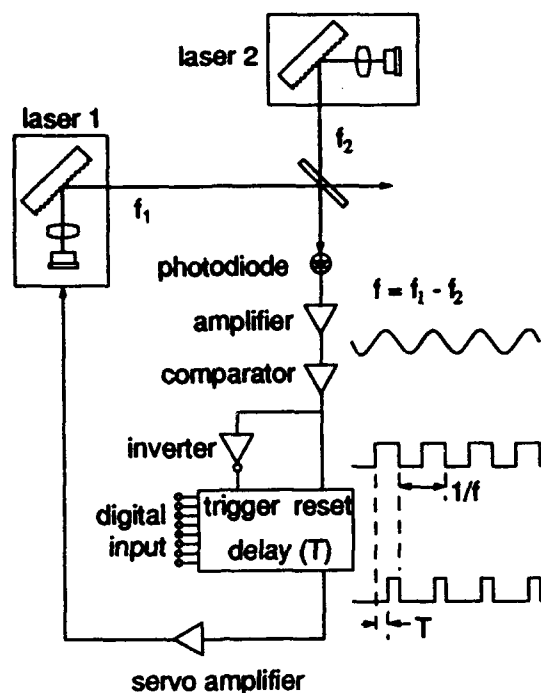
Fig. 5. Schematic of frequency-offset locking system. Not shown is the system used to stabilize laser 2 to a confocal etalon or a rubidium resonance.

Fig. 5. The frequency discriminator consists primarily of a fast comparator to convert the sinusoidal beat note into a digital signal, and a digitally controllable delay generator with delay T. The delay generator output has a duty cycle of $1/2 - fT$, where f is the frequency of the beat note. A low pass filter produces a signal proportional to the duty cycle, which thus allows linear frequency discrimination from near dc to $f = 1/2T$. Using this system, we have been able to continuously tune the offset frequency from 2-30 MHz.

These diode-laser systems allow us to produce single-mode, narrow-band radiation that may be (1) tuned over 5 -10 GHz with several hundred hertz repetition rates, (2) stabilized to an atomic resonance with excellent long-term stability, or (3) frequency offset from a second laser with a digitally-controllable offset frequency in the range of 2-30 MHz. We have taken advantage of new, higher power diodes which have become available and we now have up to 35 mW available from some of these lasers. We now have ten grating-feedback laser systems working in our laboratory.

5

We have also demonstrated a new stabilization technique for diode lasers that uses optical feedback to lock the diode laser frequency to an atomic resonance. This technique takes advantage of the high-contrast transmission spectra that can be obtained with Doppler-free saturation spectroscopy in optically thick samples.[12,13] The simple experimental set-up is depicted in Fig. 6. In this scheme, the laser beam passes through a beamsplitter and is incident into an atomic vapor cell as the pump beam. After being attenuated by the vapor, the pump beam is retroreflected and used as the counterpropagating probe beam. The probe transmission signal is monitored via the beamsplitter. The vapor cell is heated so that the atomic sample is optically thick to radiation of moderate intensity within the Doppler profile. At line center, however, the strong pump beam bleaches a hole in the sample for the weaker probe beam. With the laser optically isolated or the return beam slightly misaligned, a probe transmission spectrum such as that shown in Fig. 7, curve (b), is obtained. This spectrum resembles that of standard saturation spectroscopy (Fig. 7, curve (a)), except that the Doppler-free signal is virtually background free with the proper choice of cell temperature. Within the Doppler profile, the probe transmission resembles the transmission through an optical cavity; that is, the transmission is high on resonance and nearly zero off resonance. With the return beam aligned properly, the laser experiences optical feedback at frequencies where hole burning is effective. In the case of rubidium, optical pumping causes the dominant peaks in the spectrum to be crossover resonances between the upper-state hyperfine levels. Outside the Doppler profile, there is optical feedback that is not frequency selective. A typical probe transmission spectrum is shown in Fig. 7, curve (c). The nearly flat-topped peak at the location of one of the crossover resonances demonstrates that the laser frequency abruptly jumps onto the resonance and remains locked there while the laser would otherwise be scanning. The locking range is approximately 100 MHz. We have measured the linewidth of this stabilized laser system to be 250 kHz, more than two orders of magnitude less than the free-running linewidth.
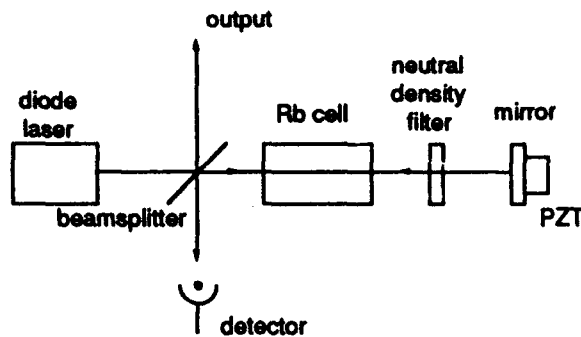
Fig. 6. Experimental schematic of diode laser stabilized with optical feedback from an optically thick rubidium cell.
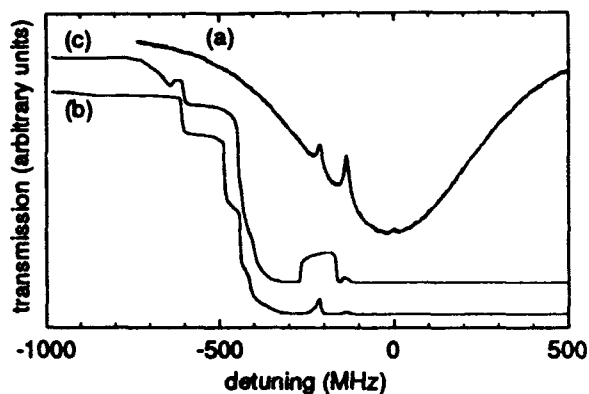
Fig. 7. Probe beam transmission spectra of the $F = 2$ to $F' = 1, 2$, and 3 hyperfine transitions of the D_2 line of ^{87}Rb. Curve (a) is a standard saturated-absorption spectrum in a room temperature cell showing the $F = 2$ to $F' = 3$ transition (at zero detuning) and two crossover resonances. Curves (b) and (c) are for the case of the optically thick rubidium cell. For curve (b) the probe beam was slightly misaligned so as to avoid optical feedback. Curve (c) shows the effect of optical feedback on the laser frequency. The curves have been displaced vertically from each other for clarity. The baselines on curves (b) and (c) represent zero probe beam transmission.

III. Rubidium atomic funnel

The atomic beam and atom interferometer are housed in a two-chamber, differentially pumped vacuum system. The source chamber is pumped with a turbomolecular pump and has a base pressure of 2×10^{-8} Torr and an operating pressure of 6×10^{-7} when the rubidium oven is heated to produce the beam. The rubidium oven has a recirculator so that rubidium can be recycled to increase the time between oven refills.[14] The atomic funnel and interferometer are housed in a high vacuum chamber that is pumped with a trapped diffusion pump and has a base pressure of 3×10^{-9} Torr. The high vacuum chamber consists of a sphere with the funnel at its center and an

adjacent cylinder for the atom interferometer. These two pieces were designed so that they can be attached in several different configurations with the pump on either chamber. This flexibility will be useful should we desire to try other possible interferometer configurations.

With this system, we have slowed a thermal rubidium beam and loaded a three-dimensional and a two-dimensional magneto-optic trap (MOT). Rubidium atoms from the oven are slowed and cooled by the scattering force from a counterpropagating laser beam tuned below the $F = 3$ to $F' = 4$ hyperfine transition of the D_2 line of ^{85}Rb. During the cooling, the laser frequency is ramped toward the resonance frequency to compensate for the decreasing Doppler shift of the decelerating atoms.[3,4] By adjusting the frequency of the laser at the end of this ramp, we can control the characteristic velocity of the cooled beam, which is important for loading the atoms into a trap.[15] A second chirped diode laser is used to counteract optical pumping of the atoms to the other hyperfine level of the ground state.

We first loaded these slow atoms into a three-dimensional MOT, which is formed by six laser beams intersecting at the center of a pair of coils used to produce a spherical quadrupole magnetic field.[16] Each pair of counterpropagating beams has opposite circular polarizations. The beams were all derived from one laser, and a second laser was again used to counteract optical pumping. The beams are tuned below resonance and provide molasses-type damping as well as a restoring force to the zero point of the magnetic field. We used this three-dimensional trap to test our laser cooling techniques and our vacuum system and then moved on to the two-dimensional funnel configuration[5,17] which will produce the slow beam needed for our interferometer.

The coils that produce the two-dimensional quadrupole magnetic field are shown in Fig. 2. The funnel is presently oriented horizontally. Three lasers at frequencies f and $f \pm \Delta f$ are used, with the laser at frequency f used for the vertical pair of beams. In the horizontal plane, the laser beams are aligned at 45°, with the two beams coming toward the funnel output beam at frequency $f - \Delta f$ and the two beams coming from behind at frequency $f + \Delta f$. This should produce a beam of atoms moving along the axis of the magnetic field with a mean velocity of $\sqrt{2} \, \Delta f \lambda$. The three lasers are each frequency-offset locked to a fourth reference laser that is stabilized to the rubidium

Fig. 8. Digitized video image of atoms in funnel.

polarization spectrometer as described above. Thus we can independently change the laser frequencies to optimize the cooling and trapping and to control the funnel beam velocity. The frequency offset locking system described above leads to a range of possible beam velocities of 2 - 33 m/s. Velocities less than 10 m/s are too strongly influenced by gravity to be used in a horizontal interferometer but could be used in a vertical geometry.

Atoms in the funnel are monitored by viewing their fluorescence with a CCD camera. Figure 8 is a digitized video image of atoms in the funnel. Structure within the line of trapped atoms may be due to inhomogeneity in the magnetic field and in the intersecting laser fields. As the difference frequency Δf is changed, atoms are seen to be concentrated at one end or the other of the funnel. Atoms that leave the funnel along the axis will enter a region with no laser fields and so will not fluoresce. To detect these atoms, we have introduced a probe laser beyond the end of the funnel. We have detected the fluorescence from atoms entering this probe region and are now characterizing the velocities and numbers of atoms.

We have also been working on an alternate means of producing a slow beam of laser cooled atoms. Instead of loading the funnel with atoms from a laser cooled beam, we would use slow atoms in the tail of the Maxwell-Boltzmann distribution in a vapor cell. This technique has

9

been demonstrated for a three-dimensional MOT,[18] but not yet for the two-dimensional funnel configuration. To test this idea, we have cooled and trapped atoms in a magneto-optic trap contained in a small rubidium vapor cell. We have used a three-dimensional spherical quadrupole field formed by two round coils, a "stretched" quadrupole formed by two rectangular coils, and most recently a pure two-dimensional field formed by two pairs of round coils. In this last configuration, we have been able to see the atoms move around when a frequency shifted laser beam is introduced, but we have not yet clearly seen a beam of atoms emerge from the trap.

IV. Grating fabrication

We have fabricated the amplitude transmission gratings to be used for the atom interferometer. We performed the work at the National Nanofabrication Facility (NNF) at Cornell University. The gratings were fabricated using the series of processing steps[6] shown in Fig. 9. A <100> oriented silicon wafer which is polished on both sides is first coated on both sides with 120 nm of silicon nitride using low pressure chemical vapor deposition (LPCVD). Free standing membranes or windows of the silicon nitride film are made by using optical lithography to pattern the back side of the wafer, reactive ion etching (RIE) in CF_4 to remove the patterned nitride, and a hot, wet etch in KOH to remove the exposed silicon. The wet KOH etches very slowly along the <111> crystal planes, producing the beveled hole. The gratings are defined on these membranes using a JEOL JBX-5DII(U) electron-beam lithography system. Before exposure, the wafer is coated on the front side with 200 nm of polymethylmethacrylate (PMMA) and a thin ($\approx$ 20 nm) layer of gold to reduce writing distortions caused by substrate charging. The grating pattern is written in successive 80-μm "fields", with computer control to ensure that the fields are properly "stitched" together. After the grating is exposed, the PMMA is developed to leave a mask. The exposed silicon nitride is then removed using a reactive ion etch which was developed to be more selective and highly directional.[6] Figure 10 shows an SEM micrograph of part of a grating with a 250-nm grating spacing.
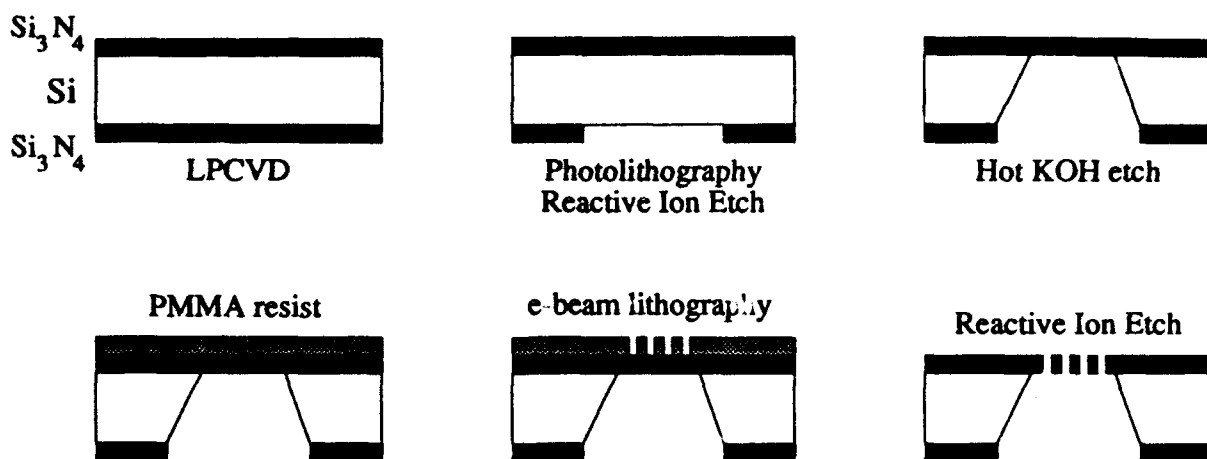
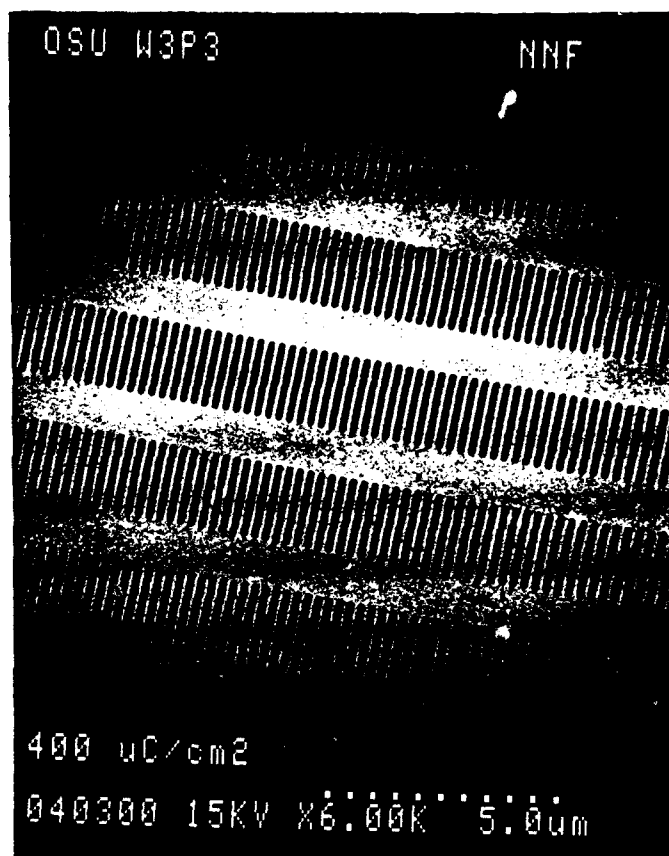**Fig. 9.** Processing steps for grating fabrication.

Fig. 10. SEM micrograph of a free-standing silicon nitride grating. The grating spacing is 250 nm and the spacing of the horizontal support bars is 4 μm.
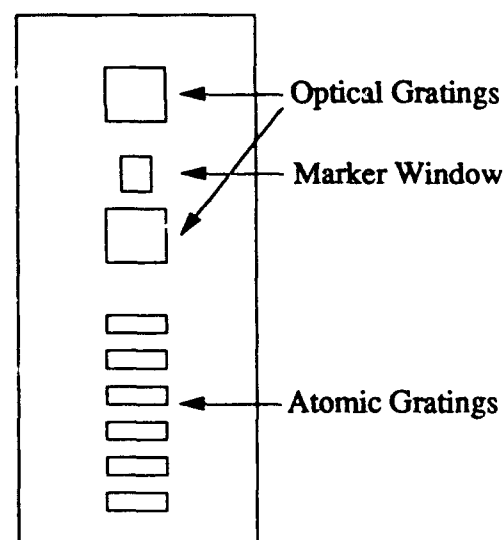
Fig. 11. Photolithographic pattern used to define free standing silicon nitride membranes.

11

We have fabricated gratings with periods of 250 nm and 500 nm and with total areas of 1 mm x 150 µm, 1 mm x 50 µm, 0.5 mm x 150 µm, and 0.5 mm x 50 µm. Each 3" wafer is divided into 20 8 mm x 18 mm chips. Each chip has six atomic scale gratings, two larger optical scale gratings, and a marker window, as shown in Fig. 11. We were not as successful with the larger optical gratings (d = 8.4 µm) as with the atomic gratings. We designed the optical gratings for use in optical alignment of the interferometer and made the windows 1 mm x 1 mm in area, thinking that we could simply scale up the atomic gratings. However, the thickness of the nitride layer was obviously not scaled up, and this led to destruction of many of the optical gratings during the last RIE step. We tried several methods and did meet with some success, though it was inconsistent.

To test the coherence of the atomic gratings we arranged for the e-beam system to write verniers on the silicon substrate. By comparing verniers written in adjacent fields, we could determine the stitching errors. We found that the fields were correctly placed to within 10 nm between subsequent fields and to within 50 nm overall. Since this is a small fraction of the 250 nm grating spacing, the gratings are quite coherent.

V. Personnel and publications

This research has been carried out with graduate students, undergraduate students, and a post-doctoral researcher. Two advanced students are working toward the Ph.D. degree; one student has received a M.S. degree and two others are nearing completion of M.S. degrees; and one undergraduate student did a senior thesis for the B.S. degree.

Details of the grating-feedback diode laser stabilization work have recently been published.[19] A paper on the optical stabilization to an atomic resonance has been submitted for publication.[20] Reports on the progress of the atom interferometer experiment have been presented at two conferences.[21,22]

References

[1] B. J. Chang, R. Alferness, and E. N. Leith, Appl. Opt. **14**, 1592 (1975).

[2] H. Mendlowitz and J. A. Simpson, J. Opt. Soc. Am. **52**, 520 (1962).

[3] W. Ertmer, R. Blatt, J. L. Hall, and M. Zhu, Phys. Rev. Lett. **54**, 996 (1985).

[4] R. N. Watts and C. E. Wieman, Opt. Lett. **11**, 291 (1986).

[5] E. Riis, D. S. Weiss, K. A. Moler, and S. Chu, Phys. Rev. Lett. **64**, 1658 (1990).

[6] D. W. Keith, R. J. Soave, and M. J. Rooks, J. Vac. Sci. Technol. B **9**, 2846 (1991).

[7] D. W. Keith, C. R. Ekstrom, Q. A. Turchette, and D. E. Pritchard, Phys. Rev. Lett. **66**, 2693 (1991).

[8] B. Dahmani, L. Hollberg, and R. Drullinger, Opt. Lett. **12**, 876 (1987).

[9] A. Hemmerich, D. H. McIntyre, D. Schropp, Jr., D. Meschede, and T. W. Hänsch, Opt. Commun. **75**, 118 (1990).

[10] C. E. Wieman and L. Hollberg, Rev. Sci. Instrum. **62**, 1 (1991).

[11] C. Wieman and T. W. Hänsch, Phys. Rev. Lett. **36**, 1170 (1976).

[12] S. Svanberg, G.-Y. Yan, T. P. Duffey, and A. L. Schawlow, Opt. Lett. **11**, 138 (1986).

[13] S. Svanberg, G.-Y. Yan, T. P. Duffey, W.-M. Du, T. W. Hänsch, and A. L. Schawlow, J. Opt. Soc. Am. B **4**, 462 (1987).

[14] M. Lambropoulos and S. E. Moody, Rev. Sci. Instrum. **48**, 131 (1977).

[15] D. Sesko, C. G. Fan, and C. E. Wieman, J. Opt. Soc. Am. B **5**, 1225 (1988).

[16] E. L. Raab, M. Prentiss, A. Cable, S. Chu, and D. E. Pritchard, Phys. Rev. Lett. **59**, 2631 (1987).

[17] J. Nellessen, J. Werner, and W. Ertmer, Opt. Commun. **78**, 300 (1990).

[18] C. Monroe, W. Swann, H. Robinson, and C. Wieman, Phys. Rev. Lett. **65**, 1571 (1990).

[19] J. J. Maki, N. S. Campbell, C. M. Grande, R. P. Knorpp, and D. H. McIntyre, Opt. Commun. **102**, 251 (1993).

[20] C. J. Cuneo, J. J. Maki, and D. H. McIntyre, submitted to Applied Physics Letters.

[21] D. H. McIntyre, H. Delfs, and T. B. Swanson, 1992 DAMOP Meeting, Chicago, Illinois, May 20-22, 1992; Bull. Am. Phys. Soc. **37**, 1139 (1992).

[22] H. Delfs, T. B. Swanson, and D. H. McIntyre, Book of Abstracts of the Thirteenth International Conference on Atomic Physics, Munich, Germany, August 3-7, 1992.